Journal of ELECTRONIC MATERIALS, Vol. 39, No. 8, 2010
DOI: 10.1007/s11664-010-1275-4
© 2010 TMS

Structural Properties of AlN Grown on Sapphire at Plasma Self-Heating Conditions Using Reactive Magnetron Sputter Deposition

HUI-CHAN SEO,[1,2] IVAN PETROV,[1,2] and KYEKYOON KIM[3,4]

1.—Department of Materials Science and Engineering, University of Illinois at Urbana-Champaign, Urbana, IL 61801, USA. 2.—Frederick Seitz Material Research Laboratory, University of Illinois at Urbana-Champaign, Urbana, IL 61801, USA. 3.—Department of Electrical and Computer Engineering, University of Illinois at Urbana-Champaign, Urbana, IL 61801, USA. 4.—e-mail: kevinkim@uiuc.edu

Aluminum nitride (AlN) films were grown on sapphire by reactive magnetron sputter deposition in N_2 discharges at plasma self-heating conditions. The growth temperature was as low as 94°C. The structural properties resulting from different substrate biases and growth pressures were investigated by atomic force microscopy, x-ray diffraction (XRD) measurements, and transmission electron microscopy (TEM). At 20 mTorr of N_2 with most sputtered species thermalized, films exhibited both AlN (0002) and $(10\bar{1}1)$ XRD peaks, with the AlN (0002) intensity initially increasing with ion energy above 15 eV, showing enhanced film quality with an optimum of 25 eV. At a lower growth pressure of 5 mTorr with energetic sputtered species, the AlN $(10\bar{1}1)$ peak disappeared and the crystallinity of AlN improved, exhibiting relaxed epitaxial AlN. The measured lattice parameter was 0.4975 nm, which was 0.10% smaller than that of bulk. The epitaxial relationship of a single-crystal AlN film was confirmed by pole figure and cross-sectional TEM. These results demonstrate that control of ion energy and energy of the sputter-deposited species is critical for film deposition at low temperature.

Key words: Aluminum nitride, sputter deposition, self-heating condition

INTRODUCTION

Wide-bandgap group III nitrides are attractive for high-temperature and high-power device applications. Among them aluminum nitride (AlN) is considered particularly useful for hard coatings, corrosion-resistant coatings, high-power microelectronics, and ultraviolet optoelectronics due to its high hardness, wide bandgap (6.2 eV), large electrical breakdown voltage, and high thermal and chemical stability.[1–3] In addition, AlN is a promising piezoelectric material for surface acoustic wave devices due to its high acoustic velocity and large piezoelectric coupling factor.[4] For all these applications, however, high-quality AlN is required. To grow such films various methods have been used including metalorganic chemical vapor deposition (MOCVD),[5] gas-source molecular-beam epitaxy (GSMBE),[6] and pulsed laser ablation,[7] all of which require high growth temperatures [T_s(MOCVD, GSMBE) ≥ 1100°C and T_s(laser ablation) ≥ 750°C] to achieve high-quality AlN. Also, due to the lack of bulk AlN substrates, heteroepitaxial growth has been employed using SiC, sapphire, and Si as the substrate, which, due to the large differences in thermal expansion coefficients of the materials, gives rise to large stress in the films leading to effects such as dislocations, wafer bowing, and cracks. The high substrate temperature is also incompatible with other processing steps required for production of semiconductor integrated circuit devices. A solution to these problems is low-temperature growth of AlN, which can be achieved

(Received August 1, 2009; accepted May 5, 2010; published online June 3, 2010)

using sputter deposition.[8,9] However, most AlN films thus deposited have been shown to be polycrystalline.[10–12]

In this work we report results of reactive magnetron sputter deposition of AlN films on sapphire substrates. The substrate was not separately heated but relied on plasma self-heating. First, the substrate temperature was measured during plasma heating. The structural properties of AlN were then examined as a function of ion energy at various substrate biases and growth pressures. High-resolution x-ray diffraction (HR-XRD) and high-resolution cross-sectional transmission electron microscopy (HR-TEM) were used to examine the film quality and epitaxial relationship.

EXPERIMENTAL PROCEDURES

AlN layers were deposited at plasma self-heating conditions to a thickness of 250 nm by using a load-locked multichamber ultrahigh-vacuum stainless-steel direct-current (DC) magnetron sputter deposition system. The target was a 6.34-cm-diameter water-cooled Al disk of 99.999% purity. The pressure in the sample introduction chamber was less than 5×10^{-8} Torr (7×10^{-6} Pa), which was achieved by using a 50 L s^{-1} turbomolecular pump (TMP). The base pressure of the main deposition chamber was 8.5×10^{-8} Torr (1.1×10^{-6} Pa), achieved by using a 500 L s^{-1} TMP. Sputtering was carried out at a constant power of 200 W and total pressure of 5 mTorr to 20 mTorr (0.67 Pa to 2.67 Pa) in N_2 (99.999%). The sapphire substrate was cleaned with successive ultrasonic rinses in trichloroethane, acetone, ethanol, and deionized water, and was blow-dried with dry N_2. A sapphire wafer was mounted on Ta platens using Mo clips. After inserting it into the sample introduction chamber, the sapphire substrate was transported to the growth chamber, where it was thermally degassed at 900°C for 2 h. Prior to deposition, the substrate was cooled to room temperature and the target was sputter-etched for 5 min for surface cleaning of the Al target metal. The deposition time was fixed at 30 min. The substrate temperature due to plasma heating was measured using a thermocouple bonded to its top surface. A pair of external Helmholtz coils with Fe pole pieces was utilized to create a uniform axial magnetic field B_{ext} in the region between the target and the substrate. This allowed us to increase or decrease the plasma density near the substrate and the self-heating temperature without decreasing the target-sputtering rate.[13] During these experiments a low ion-to-Al flux was held constant using $B_{ext} = -20$ G. Substrate bias was varied from −15 V to −35 V.

Surface roughness was measured by atomic force microscopy (AFM). AFM measurements were carried out in air using oxide-sharpened Si_3N_4 tips. To remove the tilt effect during the measurement, the images were linearly flattened. The crystal lattice parameter, quality, and orientation relationship were confirmed using $\theta/2\theta$ scan, ω scan, and pole figure. X-ray measurements were carried out using a high-resolution Philip X-pert diffractometer with a Cu $K_{\alpha 1}$ ($\lambda = 0.15406$ nm) and Ge (220) four-crystal and two-crystal monochromator in primary and secondary axes, respectively, which provided an angular beam divergence of less than 12 arcsec with a wavelength spread $\Delta\lambda/\lambda \cong 7 \times 10^{-5}$. HR-TEM analyses were carried out using a JEOL 2010F energy-filtered field-emission analytic microscope operated at 200 kV. In obtaining the diffraction pattern, the camera length used was 60 cm and the exposure time was 0.5 s. Cross-sectional specimens were prepared by mechanically grinding them to a thickness of 20 μm, and the final thinning was carried out by ion milling using a 5 keV Ar^+ ion beam incident at 10°.

RESULTS AND DISCUSSION

While varying the external magnetic field, the sapphire substrate temperature was measured using a thermocouple attached to its top surface. The total pressure was fixed at 20 mTorr. The temporal temperature profile is presented in Fig. 1. At the high ion-to-Al flux ratio J_i/J_{Al} ($B_{ext} = 180$ G) and low J_i/J_{Al} ($B_{ext} = -20$ G), the substrate temperature was 289°C and 94°C, respectively. The substrate temperature at low J_i/J_{Al} stabilized within 6 s. To deposit AlN films at the lowest growth temperature, 94°C, the ion-to-Al flux ratio was held constant using $B_{ext} = -20$ G.

An initial AlN deposition experiment was carried out as a function of substrate bias at a fixed total pressure of 20 mTorr. The ion irradiation energy (E_i) at the substrate was estimated from

$$E_i \cong e\left(\left|V_s - V_p\right|\right), \quad (1)$$

where V_s and V_p denote the substrate potential and plasma potential, respectively. The substrate potential (V_s) could be varied by applying a negative

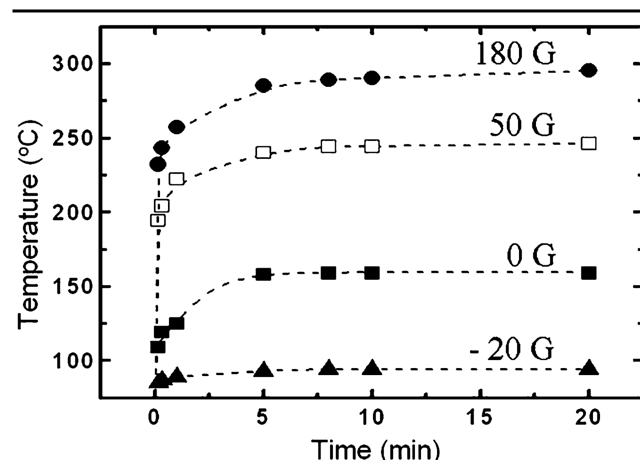

Fig. 1. Substrate temperature profile during sputtering of Al in 20 mTorr N_2 discharge as a function of external magnetic field, B_{ext}.

substrate bias between −15 V and −35 V, whilst the variation of the plasma potential (V_p) could be ignored during the deposition for constant B_{ext}.[13] The ion flux to the substrate, as determined by glow discharge mass spectroscopy measurements during reactive sputtering of metal targets in pure nitrogen atmosphere, is due primarily to N_2^+ (~96.3%), with ~3.5% of N^+.[14] The AlN growth rate (0.50 μm/h) was almost constant while the substrate bias was varied. Figure 2 shows typical $\theta/2\theta$ scans and ω-rocking curves from 250-nm-thick AlN films deposited on sapphire (0002) with V_s = −15 V, −20 V, −25 V, −30 V, and −35 V. The inset shows the full-width at half-maximum (FWHM) of AlN (0002) $\theta/2\theta$ scans ($\Gamma_{2\theta}$) and rocking curves (Γ_{ω}). The scan shows (0002) and ($10\bar{1}1$) AlN diffraction peaks at 36.12° and 37.94°, respectively. It is seen that, with increasing substrate bias, the peak intensity of AlN (0002) increased and the FWHM of AlN (0002) decreased from $I = 2.67 \times 10^3$ cts s^{-1}, $\Gamma_{2\theta}$ = 19.6 arcmin, and Γ_{ω} = 153.6 arcmin with V_s = −15 V to $I = 2.91 \times 10^4$ cts s^{-1}, $\Gamma_{2\theta}$ = 12.9 arcmin, and Γ_{ω} = 87.6 arcmin with V_s = −25 V. This indicates that, with increasing ion energy, the resulting accelerated ions will deliver a larger fraction of their energy to the film surface, promoting adatom diffusion with higher mobility, which results in smoother and higher-quality films. At V_s higher than −25 V the AlN (0002) peak intensity almost disappeared and FWHM increased to I = 77 cts s^{-1}, $\Gamma_{2\theta}$ = 18.7 arcmin, and Γ_{ω} = 201.6 arcmin with V_s = −35 V, which shows that there is an optimum ion energy for improving film quality and that too high an ion energy can degrade film quality at low growth temperature. From the 2θ value, at V_s = −25 V the lattice parameter in the growth direction was determined to be 0.4961 nm. This value is 0.38% smaller than the reported relaxed AlN lattice constant, c = 0.4980 nm,[15] indicating that the film exhibits slight in-plane tension.

Large stress can cause bowing and cracks in the film. Therefore, control of residual stress is important. The effect of pressure on the stress was investigated at the optimized substrate bias of −25 V. Figure 3 shows typical $\theta/2\theta$ scans and

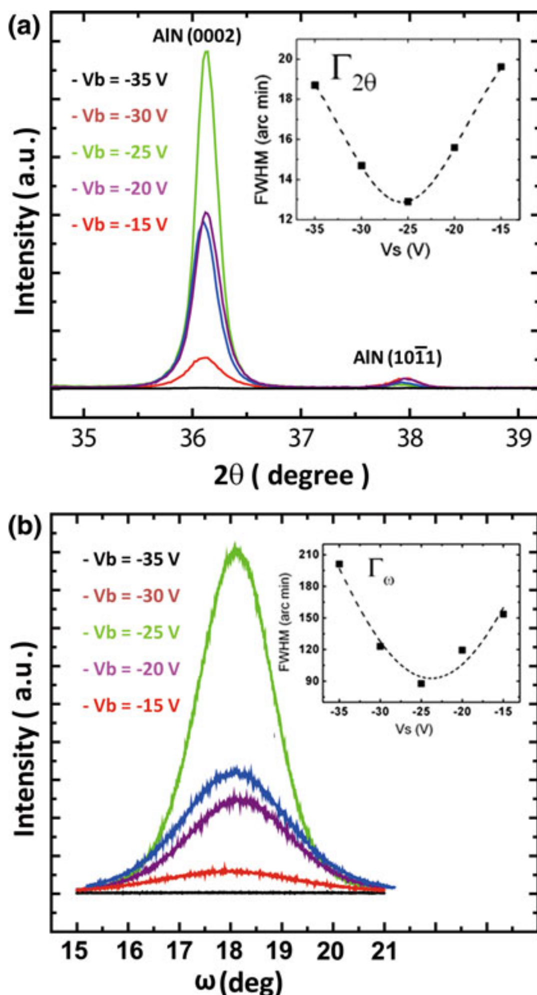

Fig. 2. HR-XRD (a) $\theta/2\theta$ scans, (b) ω-rocking curves, and FWHM (*inset*) of AlN (0002) peaks as a function of substrate bias from −15 V to −35 V at 20 mTorr.

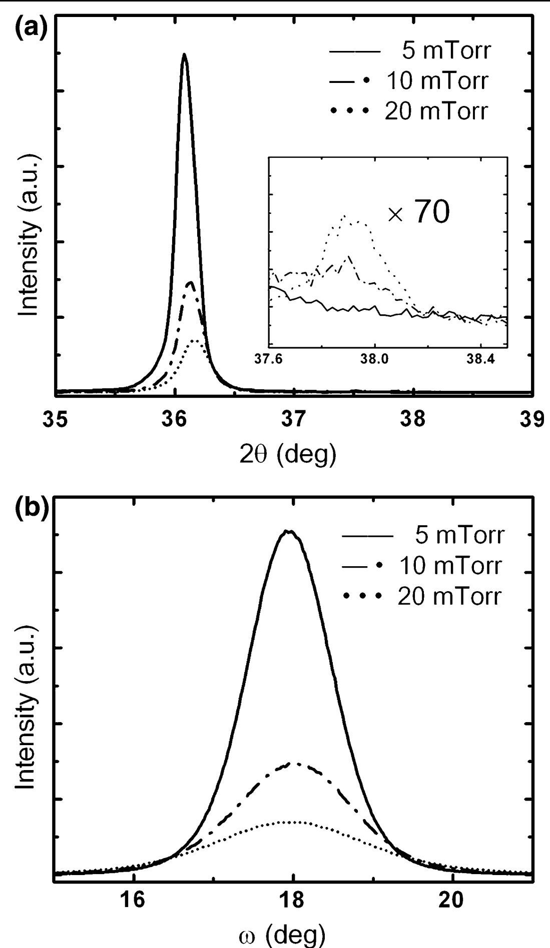

Fig. 3. HR-XRD (a) $\theta/2\theta$ scans, (b) ω-rocking curves, and FWHM (*inset*) of AlN (0002) peaks as a function of deposition pressure from 5 mTorr to 20 mTorr.

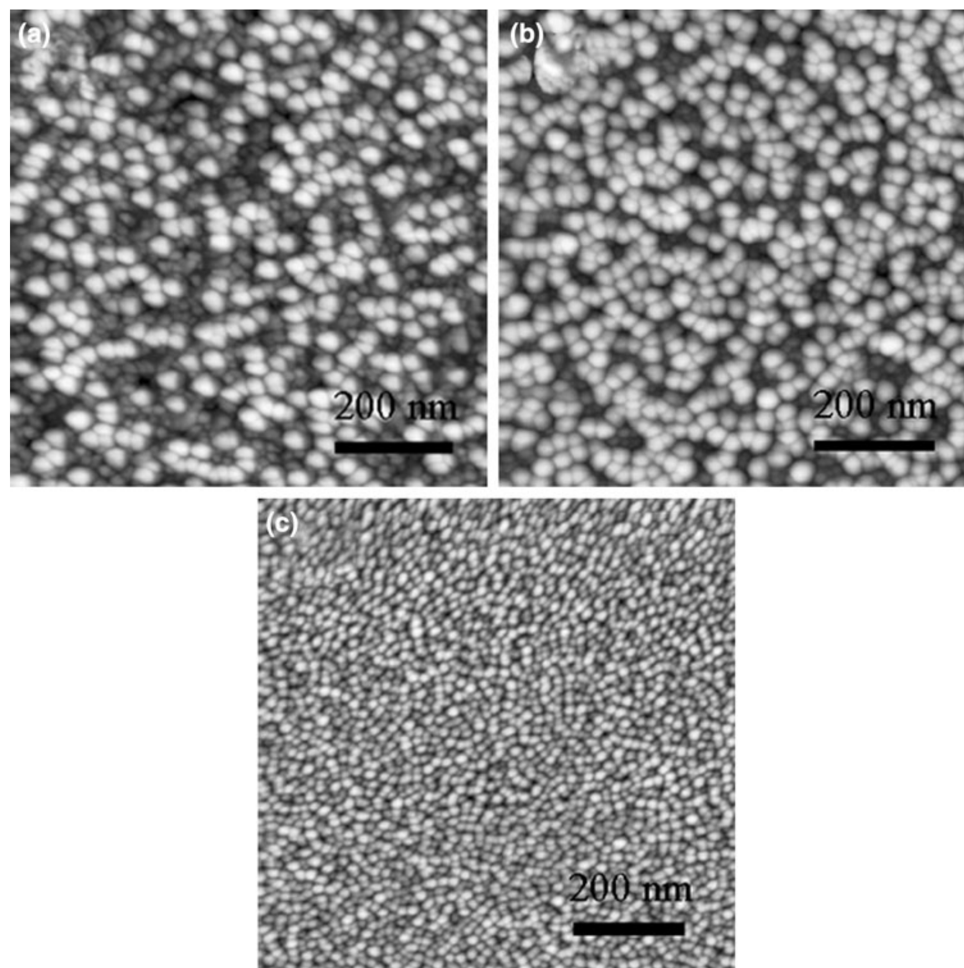

Fig. 4. AFM images of AlN films grown at deposition pressure of (a) 20 mTorr, (b) 10 mTorr, and (c) 5 mTorr. The scan area was 1 μm $\times$ 1 μm.

rocking curves from AlN (0002) at three different growth pressures. From $\theta/2\theta$ scans the lattice parameter, c, was calculated. With decreasing pressure, the lattice parameter changed from 0.4961 nm to 0.4975 nm, which corresponds to a value 0.10% smaller than the relaxed lattice constant. This shows that the film was almost relaxed at 5 mTorr. With decreasing pressure, the AlN (0002) peak intensity increased and FWHM decreased to $I = 8.98 \times 10^4$ cts s^{-1}, $\Gamma_{2\theta} = 9.9$ arcmin, and $\Gamma_{\omega} = 65.4$ arcmin at 5 mTorr. This behavior can be explained by the scattering events. At high pressure, the probability of scattering events increases and more particles lose their energy and are effectively thermalized,[16] and the tendency for film bombardment by particles at an oblique angle increases due to scattering.[17] Therefore, at high pressure, films may fail to attain high density. In contrast, at low pressure, due to less scattering, greater numbers of particles will strike the films at an angle normal to the film surface, preserving a larger portion of the sputtered energy. This effect results in denser films and more efficient atomic arrangements, giving rise to higher-quality films. The inset to Fig. 3a shows that the AlN $(10\bar{1}1)$ peak disappeared at 5 mTorr. AFM observation was carried out to investigate the surface morphology of the AlN films (Fig. 4). The film surface was seen to be covered with small grains. The root-mean-square (RMS) roughness of the films grown at 20 mTorr, 10 mTorr, and 5 mTorr were determined to be 4.33 nm, 1.60 nm, and 1.18 nm, respectively, in a 1 μm $\times$ 1 μm area, and the grain size became smaller and more uniform.

Pole figure measurement was performed on the film grown at 5 mTorr. In Fig. 5a, it is seen that there are six {102} poles ($2\theta = 49.816°$) of AlN films located at $\psi = 42°$, but that there are no other {102} poles. This indicates that the films are single crystal with sixfold symmetry of wurzite structure. The circles correspond to $\psi = 30°$, 60°, and 90°, respectively. Figure 5b shows {203} poles ($2\theta = 91.1°$) of AlN films at $\psi = 66°$. There are sapphire {315} poles near the {203} poles and the difference in ϕ is 15°, which means that there is 30° in-plane rotation of AlN with respect to the sapphire substrate and that the AlN films were epitaxially grown with the orientation relationship: $(001)_{AlN}/(001)_{Sap}$, $[1\bar{1}00]_{AlN}/[0\bar{1}10]_{Sap}$. This rotation is due to the lattice mismatch between AlN and sapphire. $[10\bar{1}0]_{AlN}$ has a

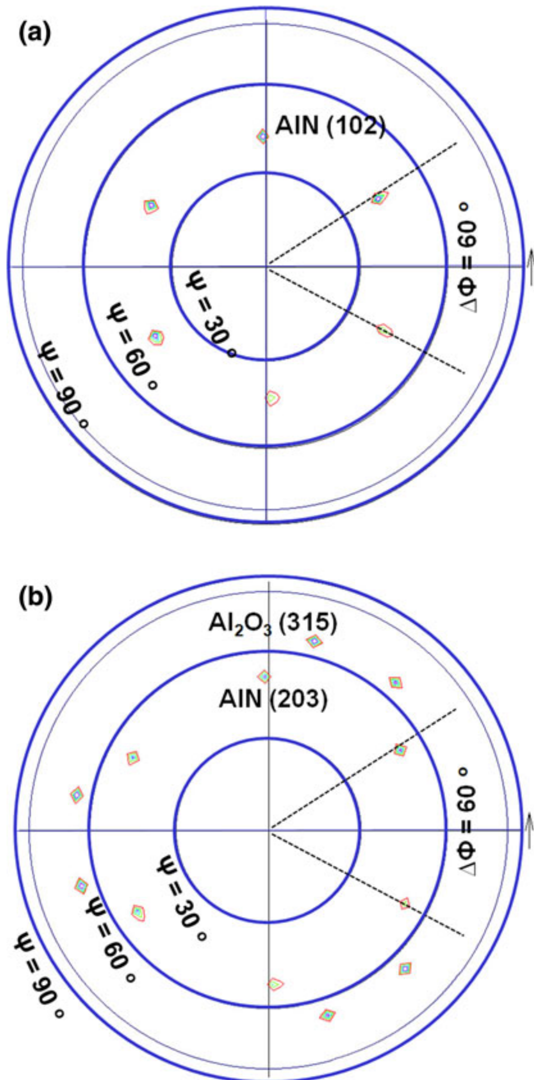

Fig. 5. (a) AlN {102} x-ray pole figure for 2θ = 49.816° and (b) AlN {203} x-ray pole figure for 2θ = 91.1°. Pole figure was recorded over the range ϕ = 0° to 360° and ψ = 0° to 85°.

very large mismatch of 34.6% with $[10\bar{1}0]_{Sap}$. However, if the AlN lattice rotates 30° about the [0001] axis, the lattice mismatch is reduced to 13.4%. Therefore, the in-plane rotation can reduce the strain energy resulting from large lattice mismatch.

Figure 6 shows HR-TEM microscopy with a selective-area diffraction (SAED) pattern from the interface between the sapphire substrate and AlN films grown at 5 mTorr. The zone axis of AlN was $[11\bar{2}0]$. The lattice fringes are continuous across the film/substrate interface, showing the epitaxial nature of the overlayer. The presence of misfit dislocations is marked by arrows, being observed every seven or eight atoms, demonstrating that the film is almost relaxed with dislocations because the lattice mismatch of AlN and sapphire is 13.4%. SAED patterns contain only symmetric single-crystal reflections arising from AlN films and sapphire. The diffraction pattern shows that AlN$(1\bar{1}00)$ and AlN(0002) are

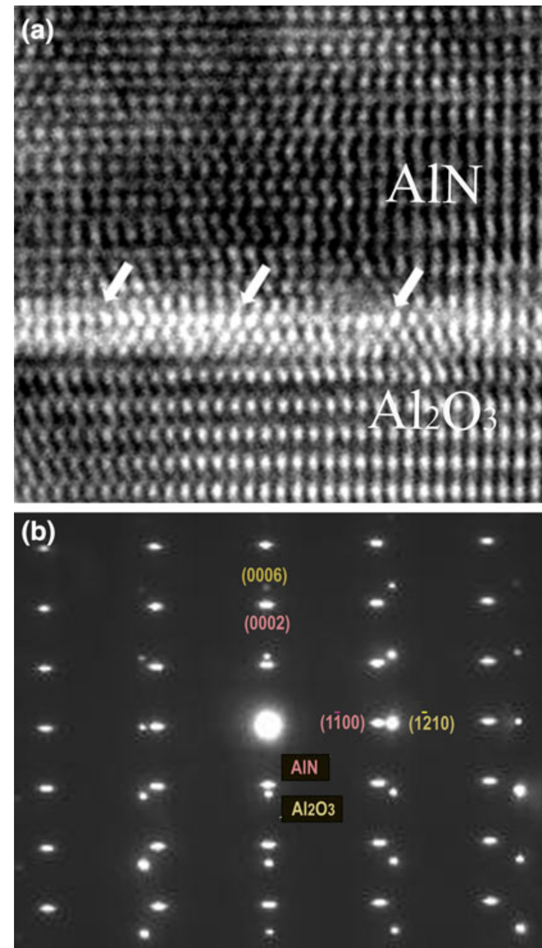

Fig. 6. (a) $[11\bar{2}0]$ zone axis cross-sectional HR-TEM image from an epitaxial AlN grown on a sapphire substrate and (b) SAED pattern from the same sample.

parallel to $Al_2O_3(1\bar{2}10)$ and $Al_2O_3(0006)$, respectively, which proves the 30° in-plane rotation of AlN films relative to the sapphire substrate.[18] This orientation relationship from the diffraction pattern is consistent with the results of the pole figure.

CONCLUSIONS

The effect of ion energy and deposition pressure on AlN films grown by reactive magnetron sputter deposition was examined. High ion energy can enhance adatom mobility; however, excessive ion energy can degrade film quality. At lower pressure, films showed better smoothness and better crystalline quality. Even at plasma self-heating condition, single crystals could be grown on sapphire substrates and the lattice parameter was 0.4975 nm, which is 0.10% smaller than the relaxed one. The overall orientation relationship was $(001)_{AlN}/(001)_{Al2O3}$, $[1\bar{1}00]_{AlN}/[0\bar{1}10]_{Al_2O_3}$.

ACKNOWLEDGEMENTS

This work was supported in part by DARPA HR0011-10-1-0050 through the University of

Illinois Frederick Seitz Materials Research Laboratory (FS-MRL), the Research Board and Grainger Center for Electric Machinery and Electromechanics of the University of Illinois, and Northrop–Grumman Space Technologies. The authors appreciate the use of the facilities of the FS-MRL Center for Microanalysis of Materials at the University of Illinois, which is partially supported by DOE. Taekyung Kim is acknowledged for his technical assistance in the TEM analysis.

REFERENCES

1. S. Nakamura, T. Mukai, and M. Senoh, *Appl. Phys. Lett.* 64, 1687 (1994).
2. N. Onojima, J. Kaido, J. Suda, and T. Kimoto, *Phys. Status Solidi C* 2, 2643 (2005).
3. S. Strite and H. Morkoc, *J. Vac. Sci. Technol. B* 10, 1237 (1992).
4. F. Engelmark, G.F. Iriarte, I.V. Katardjiev, M. Ottosson, P. Muralt, and S. Berg, *J. Vac. Sci. Technol. A* 19, 2664 (2001).
5. A.V. Lobanova, E.V. Yakovlev, R.A. Talalaev, S.B. Thapa, and F. Scholz, *J. Cryst. Growth* 310, 4935 (2008).
6. S. Iwata, Y. Nanjo, T. Okuno, S. Kurai, and T. Taguchi, *J. Cryst. Growth* 301, 461 (2007).
7. J. Keckes, S. Six, W. Tesch, R. Resel, and B. Rauschenbach, *J. Cryst. Growth* 240, 80 (2002).
8. Q.X. Guo, K. Yahata, T. Tanaka, M. Nishio, and H. Ogawa, *J. Cryst. Growth* 257, 123 (2003).
9. I. Ivanov, L. Hultman, K. Jarrendahl, P. Martensson, J.-E. Sundgren, B. Hjorvarsson, and J.E. Greene, *J. Appl. Phys.* 78, 5721 (1995).
10. H.T.G. Hentzell, J.M.E. Harper, and J.J. Cuomo, *J. Appl. Phys.* 58, 556 (1985).
11. T. Shiosaki, T. Yamamoto, T. Oda, and A. Kawabata, *Appl. Phys. Lett.* 36, 643 (1980).
12. X. Wang, K. Hipps, and U. Mazur, *Langmuir* 8, 1347 (1992).
13. I. Petrov, F. Adibi, J.E. Greene, W.D. Sproul, and W.-D. Munz, *J. Vac. Sci. Technol. A* 10, 3283 (1992).
14. I. Petrov, A.M. Myers, J.E. Greene, and J. Abelson, *J. Vac. Sci. Technol. A* 12, 2846 (1994).
15. L. Lui and J.H. Edgar, *Mater. Sci. Eng. R* 37, 61 (2002).
16. R.E. Somekh, *J. Vac. Sci. Technol. A* 2, 1285 (1984).
17. J.A. Thornton, *J. Vac. Sci. Technol. A* 4, 3059 (1986).
18. R.C. Powell, N.-E. Lee, Y.-W. Kim, and J.E. Greene, *J. Appl. Phys.* 73, 189 (1993).